

## Fabrication approach for molecular memory arrays

Chao Li, Daihua Zhang, Xiaolei Liu, Song Han, Tao Tang, and Chongwu Zhou<sup>a)</sup>  
*Department of E.E.-Electrophysics, University of Southern California, Los Angeles, California 90089*

Wendy Fan,<sup>b)</sup> Jessica Koehne,<sup>b)</sup> Jie Han, and Meyya Meyyappan  
*NASA Ames Research Center, Moffett Field, California 94035*

A. M. Rawlett, D. W. Price, and J. M. Tour<sup>a)</sup>  
*Department of Chemistry and Center for Nanoscale Science and Technology, Rice University, Houston, Texas 77005*

(Received 10 October 2002; accepted 6 December 2002)

We present an approach to tackle long-standing problems in contacts, thermal damage, pinhole induced short circuits and interconnects in molecular electronic device fabrication and integration. Our approach uses metallic nanowires as top electrodes to connect and interconnect molecular wires assembled on electrode arrays in crossbar architectures. Using this simple and reliable approach, we have revealed intriguing memory effects for several different molecular wires, and demonstrated their applications in molecular memory arrays. Our approach has great potential to be used for fast screening of molecular wire candidates and construction of molecular devices. © 2003 American Institute of Physics. [DOI: 10.1063/1.1541943]

Molecular electronics<sup>1–10</sup> has been considered to be one of the best solutions to the scaling limit problem the semiconductor industry may have to face in the next decade. The past decade has witnessed the tremendous potential through demonstrations of various molecular devices, but it has also seen great challenges in the device fabrication and integration. Self-assembled molecular wires have been used to build various sandwich structures with evaporated top electrodes;<sup>4,6</sup> however, getting stable and noninvasive top contacts has always been a problem. For example, pinhole defects existing at the domain boundaries can lead to shorted circuits during the evaporation of the top contacts, in addition to thermal damage to the monolayers. Additional difficulty lies in the fabrication complexity, as the bulk silicon micromachining technique employed to make nanopores prohibits large-scale fabrication and integration of molecular devices. The process complexity and associated low device yield are common to other approaches as well.<sup>9,10</sup> This has made it extremely difficult to perform extended research on molecular electronics on a broad interest and to construct molecular systems such as memory arrays. In this letter, we present an approach that has shown promise in solving the abovementioned problems.

Our approach is the use of metallic nanowires as top electrodes to interconnect molecular wires assembled on patterned electrode arrays in crossbar architectures. Shown in Fig. 1 is a simple example of arrays of molecular devices. We started with silicon wafers covered with 500 nm thermal oxide. Standard photolithography was first utilized to define large bonding pads and electrodes shown in Fig. 1(a). E-beam lithography was then carried out to write four parallel electrodes connected to the large electrodes, followed by evaporation of 2 nm Ti and 30 nm Au. These electrodes are typically 150 nm wide and 10 mm long, spaced by 200 nm,

as shown in Fig. 1(a) inset. The second step was to assemble molecular wires terminated with thioacetate groups (see Fig. 2) onto these nanoelectrodes to form highly ordered monolayers.<sup>12</sup> Ellipsometry was performed to measure the thickness of the film atop large gold pads to confirm the formation of the self-assembled monolayer (SAM). An atomic force microscope (AFM) was deliberately operated in the contact mode to inspect the uppermost electrode for the purpose of scratching the SAM off this electrode and exposing the gold. To make top contacts and interconnects to the self-assembled molecular wires atop the other three electrodes, we spun a suspension of pre-made Pd nanowires in dichloroethane onto our samples, followed by AFM inspection in the tapping mode. The Pd nanowires were prepared following a previously reported method.<sup>13</sup> Briefly speaking, commercial single-walled carbon nanotubes (Carbon Nanotechnologies Inc.) were sonicated into a suspension and then sparsely dispersed onto a tungsten grid (Alfa Aesar). This grid with nanotubes was then loaded into a vacuum chamber, followed by the evaporation of 2 nm Ti and 8 nm Pd while

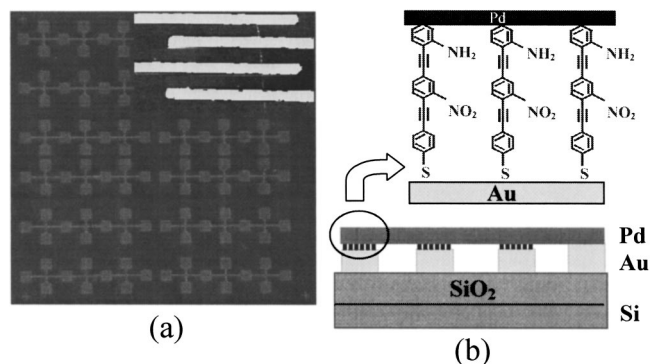


FIG. 1. (a) Optical micrograph of the nanoelectrode array. Inset: AFM image of four Au nanoelectrodes with a Pd nanowire lying across. (b) Schematic diagram of the Pd/molecular wires/Au junctions on a Si/SiO<sub>2</sub> substrate.

<sup>a)</sup>Electronic mail: chongwuz@usc.edu, tour@rice.edu

<sup>b)</sup>Also at: Eloret Corp.

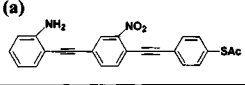
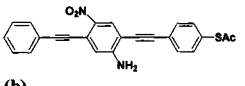
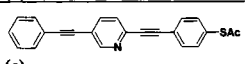
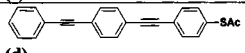
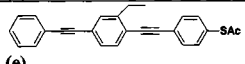
Molecular wires	Hysteresis	Retention time	On/Off ratio
(a) 	Yes	69 s	370 (-1 V)
(b) 	Yes	440 s	30 (-0.5 V)
(c) 	Yes		260 (-1.2 V)
(d) 	No		
(e) 	No		

FIG. 2. Molecular wires used. Molecules **a**, **b**, and **c** contain redox centers while molecules **d** and **e** do not contain such centers.

the grid was rotated continuously to ensure a conformal coating. Transmission electron microscopy was used to confirm the continuity and uniformity of the Pd coating. Control experiments were performed with devices consisting of Pd nanowires lying across bare gold electrodes without self-assembled molecular wires, and linear current–voltage ( $I$ – $V$ ) curves with low resistance ( $\sim 1\text{ K}\Omega$ ) were consistently observed showing no hysteresis. The Pd nanowires used in this example were typically 10–15 nm in diameter and 2–3  $\mu\text{m}$  long, and were often found to lie across all four nanoelectrodes, as shown in Fig. 1(a) inset. The final devices are arrays of Pd/molecular wires/Au sandwich structures formed at each intersection, with the uppermost electrode as a common electrode, as it formed an ohmic contact with the interconnecting Pd nanowire. A schematic diagram of our devices is shown in Fig. 1(b).

To validate this approach, we have studied extensively various molecular wire systems listed in Fig. 2. Electrical measurements were performed inside nitrogen atmosphere at room temperature. About 30% of our devices showed stable and qualitatively similar current–voltage characteristics with resistance in the range of several hundred megaohms. These devices were deemed as “good” devices exhibiting characteristics of the molecular junctions. The rest showed characteristics of open circuits, an indicator of no nanowire interconnection as confirmed via AFM inspection. Short circuits were rarely found. As a result, we usually found about 12 groups of  $3 \times 1$  arrays of molecular devices on one chip.

One of the most intriguing controversies remains as to what structural elements of the molecules give rise to memory effect and/or conductance switching. Experiments have been performed to ascertain whether the redox property (electrostatic effects of charge transfer) or the conformational change of the molecule should be responsible for the conductance switching.<sup>6,11</sup> Within this context, we synthesized five molecules as shown in Fig. 2. One of these compounds (**b**) was demonstrated before to exhibiting memory/switching behavior using the nanopore approach,<sup>6</sup> while compounds **a** and **c** are two new candidates for molecular wires. All five compounds contain similar conjugated backbones, but differ mainly on the substituent or the structure of the central part. This allows the observations to be compared and sub-

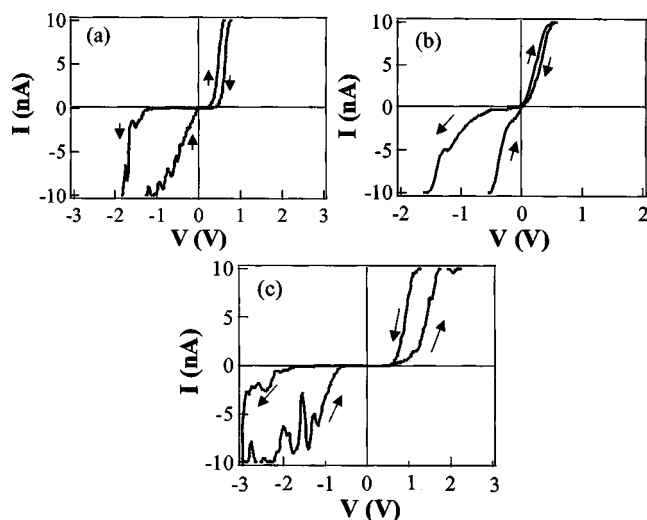


FIG. 3. Typical  $I$ – $V$  curves of molecular devices. (a), (b), and (c) correspond to molecules **a**, **b**, and **c** shown in Fig. 2, respectively.

sequently any differences in electrical behavior to possibly be ascribed to the difference in their structures. As shown in Fig. 2, molecules **a**, **b**, and **c** contain electron-retracting groups nitro or pyridine, and the nitro group is further known to have a resonance stabilizing effect. Molecule **d** is unsubstituted while **e** is substituted with a slightly electron donating group—ethyl group. Figure 3 lists three typical  $I$ – $V$  curves of devices made from molecules **a**, **b**, and **c**, respectively. The voltage was applied to the Au electrode with the Pd electrode grounded and thus negative bias corresponds to electrons injected from Au into the molecular wires. We first swept the voltage bias from 0 to a negative value, back to 0, then from 0 to a positive value and finally back to 0. Asymmetrical  $I$ – $V$  curves were observed because we used Au and Pd as the bottom and the top electrodes. In addition, pronounced hysteresis was observed with all three molecules. For example, in Fig. 3(a) the current was initially almost zero until the voltage bias reached about  $-1.2\text{ V}$ , followed by a sharp increase up to 10 nA. When the bias was swept back from  $-3$  to 0 V, the device remained rather conductive and exhibited a relatively linear  $I$ – $V$  curve with a resistance of 110 M $\Omega$  at zero bias. We define the highly conductive state as state “1” and the initially nonconductive state as the state “0.” The on/off ratio between these two states is  $\sim 370$  at  $-1\text{ V}$  bias. Hysteresis was also observed under the positive bias, though the hysteresis window appeared smaller. Similar results were also observed for molecules **b** and **c**; however, significant difference in details was also observed. Devices made of molecule **b** tend to be more conductive than devices made of molecule **a**, especially under low biases in the initial state, and this led to a smaller on/off ratio ( $\sim 30$  at  $-0.5\text{ V}$ ) observed for molecule **b**. Devices made of molecule **c** were also observed to exhibit hysteresis with an on/off ratio  $\sim 260$  at  $-1.2\text{ V}$ ; however, the  $I$ – $V$  curves were usually noisy and unstable. We suggest the reason might be related to the quality of the self-assembled monolayer, as the strong interaction between adjacent pyridine groups can lead to lower order and crystallinity in the self-assembled monolayer. In sharp contrast, devices made of molecules **d** and **e** consistently did not show any hysteresis even though more than 50 devices were measured for each compound. Further-

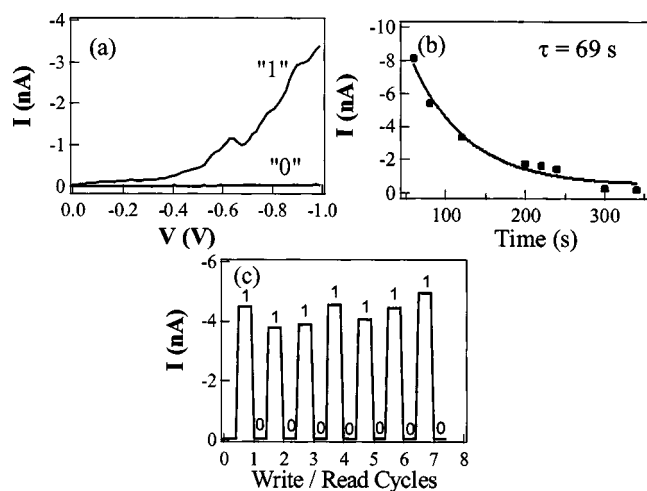


FIG. 4. (a)  $I$ - $V$  curves recorded after the device containing molecule **a** was written into states 1 and 0. (b) Retention time measurement. (c) Current recorded after the device was repeated written into states 1 and 0.

more, we also measured retention time as further described below. We summarize some major results in Fig. 2. First, we confirm a direct correlation of redox group to memory effect and conductance switching. Second, the on/off ratio and retention time vary for devices made of different wires showing memory effects. It has to do with effects of conformational and/or packing structures as well.

The above work on a fabrication approach to different molecular wires enables a quick demonstration of memory array devices. We have also performed detailed measurements to assess the memory performance of devices made of molecules **a**, **b**, and **c**. Here we concentrate on the write/read characteristics of molecule **a**. We have found that the device can be written into state 1 by applying a  $-3$  V bias or voltage pulse no matter whether the initial state is 0 or 1, and similarly this device can be written into state 0 by a  $3$  V bias or voltage pulse. A small bias, usually below  $-1$  V, can be utilized to read the state without altering the information stored. Figure 4(a) shows two  $I$ - $V$  curves after the devices were written into states 1 and 0, respectively. One can clearly see the state 1 is highly conductive, whereas state 0 offers almost no conduction. Over time we found that state 1 can slowly decay into state 0, as shown in Fig. 4(b), where black squares correspond to current values taken at  $-1$  V at various times after the device was written into state 1. These data points can be fitted with an expression  $Ae^{t/\tau}$  and a retention time constant of  $69$  s can be obtained. A retention time constant of  $440$  s was obtained for devices made of molecules **b**. Repeated writing/reading were also performed with a device containing molecule **a**, as shown in Fig. 4(c). Alternating  $-3$  and  $3$  V biases were used to write the device into states 0 and

1 and, after each writing, the device was read using a bias of  $-1$  V. The current values obtained from the reading process were plotted against the number of write/read cycles in Fig. 4(c). The state 1 was always highly conductive while the state 0 remained nonconductive. Both states are stable and reproducible, and can be easily distinguished as the on/off ratio is more than two orders of magnitude. We have also tested repeated writing/reading on devices made of molecule **b**. These devices show no significant degradation after several hundred cycles of writing and reading.

In conclusion, we have demonstrated a method to make molecular memory arrays. Our method employs metallic nanowires to work as both the interconnects and the top electrodes, thus eliminating the thermal damage problem encountered using the evaporation method. Memory effects were observed with several kinds of molecular wires containing redox centers such as pyridine and  $\text{NO}_2$  groups. Our typical devices exhibit on/off ratios around 370, retention time  $\sim 69$  s and can be repeatedly written and read without significant degradation. Our method can be extended to study other molecular systems for fast screening of molecular wire candidates.

This work is supported by USC, NASA Contract No. NAS2-99092, NSF CAREER award, NSF NER program and a Zumberger award. Work by W.F. and J.H. is supported by a NASA contract to Eloret.

<sup>1</sup>A. Aviram and M. R. Ratner, Chem. Phys. Lett. **29**, 277 (1974).

<sup>2</sup>M. A. Reed, C. Zhou, C. J. Muller, T. P. Burgin, and J. M. Tour, Science **278**, 252 (1997).

<sup>3</sup>R. M. Metzger, J. Mater. Chem. **10**, 55 (2000).

<sup>4</sup>J. Chen, M. A. Reed, A. M. Rawlett, and J. M. Tour, Science **286**, 1550 (1999).

<sup>5</sup>C. P. Collier, G. Mattersteig, E. W. Wong, Y. Luo, K. Beverly, J. Sampaio, F. M. Raymo, J. F. Stoddart, and J. M. Heath, Science **289**, 1172 (2000).

<sup>6</sup>M. A. Reed, J. Chen, A. W. Rawlett, D. W. Price, and J. M. Tour, Appl. Phys. Lett. **78**, 3735 (2001).

<sup>7</sup>X. D. Cui, A. Primak, X. Zarate, J. Tomfohr, O. F. Sankey, A. L. Moore, T. A. Moore, D. Gust, G. Harris, and S. M. Lindsay, Science **294**, 571 (2001).

<sup>8</sup>L. A. Bumm, J. J. Arnold, M. T. Cygan, T. D. Dunbar, T. P. Burgin, L. Jones II, D. L. Allara, J. M. Tour, and P. S. Weiss, Science **271**, 1705 (1996).

<sup>9</sup>J. Park, A. N. Pasupathy, J. I. Goldsmith, C. Chang, Y. Y. Yaish, J. R. Petta, M. Rinkoski, J. P. Sethna, H. D. Abruña, P. L. McEuen, and D. C. Ralph, Nature (London) **417**, 722 (2002).

<sup>10</sup>W. Liang, M. P. Shores, M. Bockrath, J. R. Long, and H. Park, Nature (London) **417**, 725 (2002).

<sup>11</sup>Z. J. Donhauser, B. A. Mantoosh, K. F. Kelly, L. A. Bumm, J. D. Monnell, J. J. Stapleton, D. W. Price, A. M. Rawlett, D. L. Allara, J. M. Tour, and P. S. Weiss, Science **292**, 2303 (2001).

<sup>12</sup>J. M. Tour, A. M. Rawlett, M. Kozaki, Y. Yao, R. C. Jagessar, S. M. Dirk, D. W. Price, M. A. Reed, C. Zhou, J. Chen, W. Wang, and I. Campbell, Chem.-Eur. J. **7**, 5118 (2001).

<sup>13</sup>Y. Zhang and H. Dai, Appl. Phys. Lett. **77**, 3015 (2000).